

Reconstruction of $f(R)$ gravity with ordinary and Entropy-corrected (m,n) -type Holographic dark energy model

Prabir Rudra¹

Department of Mathematics, Asutosh College, Kolkata-700 026, India.

Abstract

In this assignment we will present a reconstruction scheme between $f(R)$ gravity with ordinary and entropy corrected (m,n) -type holographic dark energy. The correspondence is established and expressions for the reconstructed $f(R)$ models are determined. To study the evolution of the reconstructed models plots are generated. The stability of the calculated models are also investigated using the squared speed of sound in the background of the reconstructed gravities.

Keywords: Dark energy, Dark matter, Modified gravity, Holographic, Entropy, Reconstruction.

Pacs. No.: 98.80.-k, 98.80.Es, 95.35.+d, 95.36.+x

1 Introduction

The acceleration of the universe, as confirmed by various cosmological observations such as Ia type supernovae, CMB, WMAP, etc. has been the greatest cosmological discovery over the last 50 years [1, 2, 3]. In the background of the classical Newton's theory of gravitation, this seemed to be quite an unusual and unexpected phenomenon. The reason behind this can be attributed to the fact that the classical theory does not give us any idea regarding the repulsive nature of gravity which is quite evident from the accelerated expansion of the universe. As a possible explanation to the phenomenon, scientists resorted to a mysterious negative pressure component named the dark energy. Instead of competition from other counterparts such as the theory of modified gravity, dark energy has gained popularity of the last decade. Nevertheless, dark energy and modified gravity theory complements each other as is evident from literature [4, 5, 6]. Observations suggest that almost two-thirds of the total energy of the universe is contributed by this mysterious form of energy. The rest of the portion is occupied by dark matter with a little contribution from baryonic matter [7].

In the quest of a quantum gravity theory, Fischler and Susskind [8, 9] proposed the holographic principle. In accordance with the holographic principle the dark energy in the context of quantum gravity is known as the holographic dark energy (HDE). Cohen et al. [10] proposed an enlargement relationship between the infra-red (IR) and ultraviolet cut-offs. The relationship is basically due to the limitation set by the formation of a black hole, which establishes an upper limit for the vacuum energy, $L^3 \rho_v \leq LM_P^2$, where ρ_v is the HDE density related to the UV cut-off, L is the IR cut-off and M_P is the reduced Planck mass. Over the years various dark energy that have been developed which remain plagued with different cosmological problems. The notable ones being the cosmic coincidence problem, fine tuning problem, etc. It must be noted that HDE may provide simultaneous natural solutions to both dark energy and cosmological problems [11]. Precisely, it gives excellent solutions to the coincidence problem [12] and the phantom crossing [13]. The novel feature of the model is that it has reasonable agreement with the astrophysical data of CMB, SNeIa and galaxy redshift surveys [14]. As a result scientists have been inclined to extend the idea of HDE dark energy via various prescriptions. Extensions using different cut-offs is done in the ref. [15] and various entropy corrections have been considered in [16]. The holographic scale denoted by L has a direct relation with the future event horizon [11], the conformal age of the universe [17] or the Ricci scalar of the universe [18]. The model taking into account the conformal age of the universe is widely known as new agegraphic dark energy (NADE) model in literature. Recently an extension

¹prudra.math@gmail.com

to this idea has been introduced by the name of (m, n) -type HDE [19], where m and n are the parameters associated with the chosen IR cut-off given by,

$$L = \frac{1}{a^m(t)} \int_0^t a^n(t') dt' \quad (1)$$

If we consider the consistency of a HDE model with a conformal-like age of the universe as the scale L with the past inflationary phase, perhaps the direct physical motivation of proposing such characteristic scales for the (m, n) -type holographic dark energy model is still obscure. In spite of such theoretical difficulty the model has some significant advantages that propelled its survival. The model generalizes the theory with noteworthy improvements. Moreover the parameters (m, n) opens up space to fit observational data in the background of a sound theoretical framework.

It is seen that various cosmological scenarios can be achieved by giving some specific values to (m, n) . The transition of the Equation of state (EoS) across the phantom divide can easily be achieved for some particular values of (m, n) even without the introduction of any interaction between dark energy and dark matter. Similarly for suitable values of (m, n) , all the agegraphic-like dark energy models can be recovered. For age-like holographic models, when $m = n$ it seems that dark energy behaves as the dominant ingredient in the early epochs of the universe. This implies the unification of dark energy with dark matter. But we need to introduce some mechanism that can differentiate dark energy from the dark matter state in the early epoch and help us to identify the dominating nature of dark energy in the late universe, which will ultimately drive the acceleration of the universe. An appropriate interaction between dark energy and dark matter serves the purpose. The stability of the model in the dark energy dominated era has already been confirmed. In ref. [24] it is seen that, best-fit analysis with observational data indicates that this model with $m = n + 1$ and small m is more favoured and physically more viable.

From literature, we know that a suitable alternative to the concept of dark energy in justifying the late cosmic acceleration lies in the modification of the theory of gravity, i.e, modifying the Einstein-Hilbert action. A popular way is to use an analytic function $f = f(R)$ in place of R in the action, where R is the Ricci scalar [25, 26]. The modification basically deals with the geometry of space-time and is responsible for varying its curvature. In this connection it must be noted that $f(R) \propto R^2$ kind of theories could successfully generate inflationary scenario for the early universe [27]. Since the curvature R decreases as the universe evolves, any inverse power of R in the expression of $f(R)$ will generate a late time accelerating universe. Detailed description of $f(R)$ theories can be widely found in literature [28, 29]. Although most of the works in literature deal with the present day acceleration, yet recently some works can be found where the authors have considered the smooth transition from decelerated to an accelerated regime [6]. Moreover it has been a challenge to realize both the early time inflation and the late time acceleration from the standard $f(R)$ gravity models. However in this regard some light has been thrown in ref. [30, 31]. Recently reconstruction scheme has been a very interesting topic of study in cosmology. Reconstruction scheme has been studied using $f(R)$ gravity on many occasions by different authors [32]. In ref. [23] the authors have discussed a reconstruction scheme of $f(G)$ gravity with (m, n) -type and entropy corrected (m, n) -type HDE models. Motivated by this, we set to develop a reconstruction scheme between $f(R)$ gravity and two types of HDE models, namely the (m, n) -type HDE model and entropy corrected (m, n) -type HDE (ECHDE) model in this assignment.

The Einstein field equations in the FRW model in the background of $f(R)$ gravity are discussed in section 2. Reconstruction scheme with (m, n) -type HDE and entropy corrected (m, n) -type HDE is studied in section 2.1 and 2.2 respectively. The stability of the reconstructed models is discussed in section 3. Finally the paper ends with a conclusion in section 4.

2 Reconstruction in $f(R)$ gravity

The generalized Einstein-Hilbert action for $f(R)$ gravity is given by,

$$S = \int \left[\frac{1}{16\pi G} f(R) + \mathcal{L} \right] \sqrt{-g} d^4x \quad (2)$$

where R is replaced by $f(R)$ in the Einstein-Hilbert action. Here $f(R)$ is an analytic function of R and \mathcal{L} is the usual matter field Lagrangian. The corresponding field equations in FRW space-time is given by,

$$3 \frac{\dot{a}^2}{a^2} = \frac{\rho_m}{f_R} + \frac{1}{f_R} \left[\frac{1}{2} (f(R) - Rf_R) - 3\dot{R}f_{RR} \frac{\dot{a}}{a} \right] \quad (3)$$

and

$$2\frac{\ddot{a}}{a} + \frac{\dot{a}^2}{a^2} = -\frac{1}{f_R} \left[\ddot{R}f_{RR} + \dot{R}^2 f_{RRR} + 2\dot{R}f_{RR}\frac{\dot{a}}{a} - \frac{1}{2}(f(R) - Rf_R) \right] \quad (4)$$

where dots and primes denote derivative with respect to cosmic time and R respectively. Here ρ_m is the dark matter density, and the corresponding pressure p_m is taken to be zero. So we can write the contribution by curvature to density and pressure as,

$$\rho_R = \left[\frac{1}{2}(f(R) - Rf_R) - 3\dot{R}f_{RR}\frac{\dot{a}}{a} \right] = \frac{1}{2}(f(R) - Rf_R) + 18 \left(\ddot{H} + 4H\dot{H} \right) Hf_{RR} \quad (5)$$

and

$$p_R = \left[\ddot{R}f_{RR} + \dot{R}^2 f_{RRR} + 2\dot{R}f_{RR}\frac{\dot{a}}{a} - \frac{1}{2}(f(R) - Rf_R) \right] \quad (6)$$

where $R = -6 \left(\dot{H} + 2H^2 \right)$ and $\dot{R} = -6 \left(\ddot{H} + 4H\dot{H} \right)$.

2.1 Reconstruction with (m,n)-type HDE model

The energy density of the (m, n) -type HDE model as given by ref. [19] is,

$$\rho_v = \frac{3b^2}{L^2} \quad (7)$$

where b is a constant and L is the generalized IR cut-off defined as,

$$L = \frac{1}{a^m(t)} \int_0^t a^n(t') dt' \quad (8)$$

where m and n are constants.

A simple calculation gives

$$\dot{L} = -mHL + a^{n-m}(t) \quad (9)$$

Now we establish the correspondence by setting $\rho_v = \rho_R$. We get,

$$\frac{1}{2}(f(R) - Rf_R) + 18 \left(\ddot{H} + 4H\dot{H} \right) Hf_{RR} = \frac{b^2}{L^2} \left(\frac{2a^{n-m}}{HL} - 2m - 3 \right) \quad (10)$$

where f_R and f_{RR} are respectively the first and second order derivatives of $f(R)$ with respect to R . We consider the scale factor as the power law form of time $a(t) = a_0 t^p$, where p is a positive constant.

The above is a differential equation of second order. Solving this we get,

$$\begin{aligned} f(R) = & \frac{A}{6} a_0^{-3n} \left(6^{p/2} a_0 \left(\frac{B}{R} \right)^{p/2} \right)^{-m} \left(\frac{B}{R} \right)^{3(m-n)p/2} \left[\exp(-p/2) \left(-4a_0^{3m} b^2 \exp(p/2) \sqrt{B/p} (1 + np)^3 \times \right. \right. \\ & \left. \left(6^{p/2} a_0 (B/R)^{p/2} \right)^n R + 2a_0^{2m+n} b^2 \exp(p/2) \sqrt{Bp} \left(2A^{-1/3} m (1 + np)^2 + 3A^{-1/3} (1 + 2np + n^2 p^2) \right) \times \right. \\ & \left. \left(6^{p/2} a_0 \frac{B^{p/2}}{R} \right)^m \left(\frac{B}{R} \right)^{(n-m)p/2} R - 6a_0^{3n} p^2 \left(6^{p/2} a_0 \frac{B^{p/2}}{R} \right)^m \left(\frac{B}{R} \right)^{3(n-m)p/2} C_1 \frac{\exp(p/2)}{A} (1 - 2p)^2 \right. \\ & \left. - \exp(1/4) \sqrt{B/p} C_2 \left(-\frac{1}{A} + \frac{2p}{A} \right) \right] + \frac{3C_2}{A} a_0^{3n} \sqrt{\pi} \left(6^{p/2} a_0 \left(\frac{B}{R} \right)^{p/2} \right)^m \left(\frac{B}{R} \right)^{2+3(n-m)p/2} R^2 \times \\ & \left. Erfi \left(\frac{1}{2} \sqrt{\frac{B}{p}} \right) \right] \quad (11) \end{aligned}$$

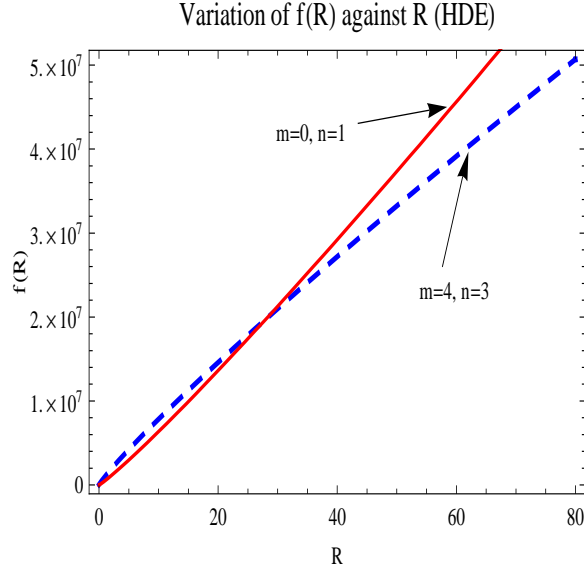


Fig.1

Fig 1 shows the evolution of $f(R)$ gravity against the Ricci scalar R for HDE dark energy for different values of m and n . The other parameters are considered as $p = 0.1, a_0 = 1, b = 1, C_1 = 2, C_2 = 3$.

where $A = 6^{\frac{3}{2}(m-n)p}$, $B = p(1-2p)$ and $Erfi$ represents the imaginary error function. C_1 and C_2 are constants of integration.

Evolution of $f(R)$ against R for the HDE model is plotted in fig.1 for two different sets of parametric values ($m = 4, n = 3$ and $m = 0, n = 1$). From literature [24] the best-fit analysis indicates that the models with $m = n + 1$ and relatively small values of m is more favoured. This includes the cases of $(m, n) = (1, 0), (2, 1), (3, 2), (4, 3)$, etc. For the purpose of study, here we choose two different pairs of parametric values, one following the above rule ($m = 4, n = 3$) and the other violating it ($m = 0, n = 1$). The idea is to compare the results in the two cases. From the figure it is seen that $f(R)$ increases with R for both set of values of m and n . For $m = 4, n = 3$, we see that $f(R)$ varies linearly with R . But for $m = 0, n = 1$, $f(R)$ follows a non-linear relation in R . The two curves intersect at around $R = 30$.

2.2 Reconstruction with entropy corrected (m,n)-type HDE model

Considering the corrected entropy-area relation with derivation of HDE, we can obtain the energy density of the entropy-corrected (m, n)-type HDE as,

$$\rho_V = \frac{3c^2}{L^2} + \frac{\xi}{L^4} \log L^2 + \frac{\zeta}{L^4} \quad (12)$$

where c, ξ and ζ are dimensionless constant and IR cutoff as considered in eqn.(1). Here also to develop the reconstruction scheme we have to consider $\rho_R = \rho_V$, which gives,

$$\frac{1}{2} (f(R) - Rf_R) + 18 (\ddot{H} + 4H\dot{H}) H f_{RR} = \frac{3c^2}{L^2} + \frac{\xi}{L^4} \log L^2 + \frac{\zeta}{L^4} \quad (13)$$

Now we consider a power law form of scale factor $a = a_0 t^p$, p being a positive constant, as considered in the previous case. Solving the above differential equation we get,

$$f(R) = \frac{1}{36} \left[36C_3 E + \frac{18e^{-p/2} C_4}{E} \left\{ 2e^{1/4} E - E^2 e^{p/2} \sqrt{\pi} Erfi(E/2) \right\} + \frac{1}{R} 2^{1-2np} 9^{-np} a_0^{2(m-2n)} (1+np)^2 \times \right. \\ \left. (pE^2/R)^{2(-1+p(m-n))} \left(2^{1+(m+n)p} 3^{2+(m+n)p} a_0^{2n} c^2 E^2 p (pE^2/R)^{(n-m)p} + a_0^{2m} F\zeta R \right) \right]$$

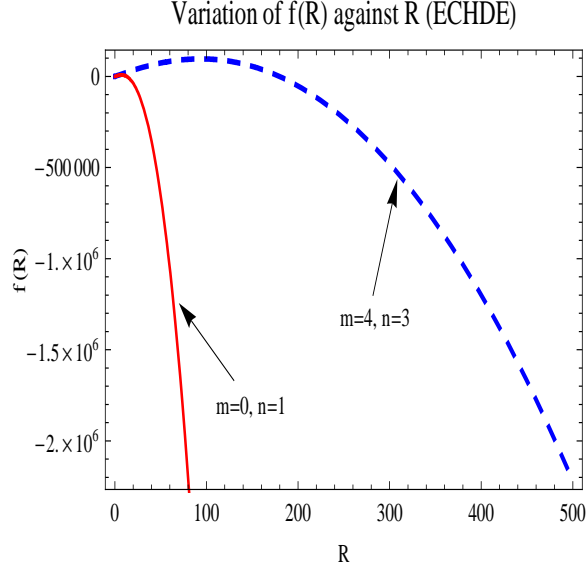


Fig.2

Fig 2 shows the evolution of $f(R)$ gravity against the Ricci scalar R for ECHDE dark energy for different values of m and n . The other parameters are considered as $p = 0.1, a_0 = 1, c = 10, C_3 = 1, C_4 = 1, \xi = 1, \zeta = 5$.

$$+ a_0^{2m} F \xi R \log \left[\frac{6^{1-mp+np} a_0^{2(n-m)} (E^2 p/R)^{1+p(n-m)}}{(1+np)^2} \right] \quad (14)$$

where $E = \sqrt{1-2p}$, $F = 36^{mp} + 2^{1+2mp} 9^{mp} n p + 36^{mp} n^2 p^2$. C_3 and C_4 are constants of integration.

Evolution of $f(R)$ against R for the ECHDE model is plotted in fig.2 for two different sets of parametric values ($m = 4, n = 3$ and $m = 0, n = 1$). From the figure it is seen that $f(R)$ decays with R for both set of values of m and n . For $m = 0, n = 1$, the curve drops steeply as compared to the curve corresponding to the values $m = 4, n = 3$, both following non-linear evolution.

3 Stability Analysis

The squared speed of sound $v_s^2 = \frac{\dot{p}}{\rho}$ is the parameter that helps us to study the stability of the background evolution of a particular gravity model. The positive value of v_s^2 characterizes stability of the corresponding model [20, 21]. The new HDE model in an interacting scenario produces a negative v_s^2 , thus exhibiting classical instability [20]. Choosing the future event horizon as IR cut-off, the squared speed of sound is found to stay in the negative level for HDE, whereas for Chaplygin gas and tachyon model, we get non-negative values of v_s^2 [22]. In ref. [21], it is observed that the perfect fluid for agegraphic dark energy is classically unstable.

In this study we have calculated v_s^2 and plotted it against cosmic time t for both the reconstructed $f(R)$ models. In fig.3, for HDE, we see that for $m = 4$ and $n = 3$, v_s^2 stays in the negative level as the universe evolves with time. The ordinate line corresponding to $t = 9$ is un-physical and so we do not include it in our discussion. So for this case we witness a classical instability of the model. In fig.4, we have generated the v_s^2 vs t plot for parametric values $m = 0, n = 1$. The asymptotic nature of the curve above the t axis implies that the squared speed of sound remains in the positive level throughout the evolution. So here we see that the model is stable. In figs.5 and 6, plots of have been generated for v_s^2 for ECHDE. In fig.5, it is seen that for $m = 4$ and $n = 3$, v_s^2 stays in the negative level for greater part of the evolution. It is to be noted that the curve undergoes a transition from positive to negative level at some time relatively in early universe. This is a contrast to what we obtained in case of HDE for the corresponding case. Unlike that case, here we get a stable model in the

early universe, but as the universe evolves, the model becomes unstable. Here we speculate that the late cosmic acceleration plays a big role in destabilizing the evolution of the universe, which is expected from general notion of dynamics. In fig.6, for $m = 0, n = 1$, we see that the model exhibits a perfectly stable nature. From the above discussion, we see that the stability of our models is parameter dependent.

In [23], the correspondence have been obtained between $f(G)$ gravity and dark energy models HDE and ECHDE. For both the HDE and ECHDE case, we have obtained a complete contrast with the study in ref [23]. From the previous studies of reconstruction scheme [20, 22] using HDE it was seen that classical instability characterized the models. So if we consider them and compare them with this assignment, it is quite obvious that $m = 4, n = 3$ is the better choice of parameters, which follows the $m = n + 1$ rule [24]. This set of parameters also give an unstable model for ECHDE.

4 Conclusion

Here we have discussed the reconstruction scheme of the $f(R)$ gravity theory with two different dark energy models, namely, (m, n) -type holographic dark energy (HDE) and entropy corrected (m, n) -type holographic dark energy (ECHDE). Power law form of scale factor has been taken into account. Using the correspondence between the gravity and dark energy we have calculated the explicit forms of $f(R)$ in terms of R for both the dark energy models. To study the nature of the calculated models plots have been generated. It is seen that for HDE case, the reconstructed model grows with R , whereas for the ECHDE case, the model decays. The result is in agreement with previous works found in literature [23]. Moreover, from literature [24] the best-fit analysis indicates that the models with $m = n + 1$ and relatively small values of m is more favoured. In our analysis we tried to justify/injustify the above fact by adopting a value satisfying the above rule and a value violating it. Our results justified the rule as the parametric values satisfying the rule produced more physically justifiable results. Moreover the stability of the reconstructed models have been brought under the scanner using the squared speed of sound in each case for two different sets of values of the parameters m and n . In the HDE case it is seen that for $m = 4, n = 3$, the model exhibits classical instability, but for $m = 0, n = 1$ the model is perfectly stable. For ECHDE case, when $m = 4, n = 3$, we witness a transition from stable to unstable state. But for $m = 0, n = 1$, the model is absolutely stable.

Acknowledgements

The author sincerely acknowledges the facilities provided by the Inter-University centre for Astronomy and Astrophysics (IUCAA), Pune, India where a part of the work was carried out. The author also acknowledges the anonymous referee for enlightening comments that helped to improve the quality of the manuscript.

References

- [1] S. J. Perlmutter et al. :- *Nature* **391** 51 (1998).
- [2] A. G. Riess et al. [Supernova Search Team Collaboration] :- *Astron. J.* **116** 1009 (1998).
- [3] D. N. Spergel et al. :- *Astrophys. J. Suppl. Ser.* **170** 377 (2007).
- [4] K. Bamba et al. :- *Phys. Lett. B* **679** 282 (2009).
- [5] K. Bamba et al. :- *Phys. Rev. D* **79** 083014 (2009).
- [6] S. Nojiri, S. D. Odintsov :- *Phys. Rev. D* **74** 086005 (2006).
- [7] SDSS Collaboration (C.L. Bennet et al.) :- *Astrophys. J.* **583** 1 (2003).
- [8] W. Fischler et al. :- *arXiv:hep-th/9806039* (1998).
- [9] L. Susskind, :- *J. Math. Phys.* **36** 6377 (1995).
- [10] A. G. Cohen et al. :- *Phys. Rev. Lett.* **82** 4971 (1999).
- [11] M. Li :- *Phys. Lett. B* **603** 1 (2004).
- [12] D. Pavon et al. :- *Phys. Lett. B* **628** 206 (2005).

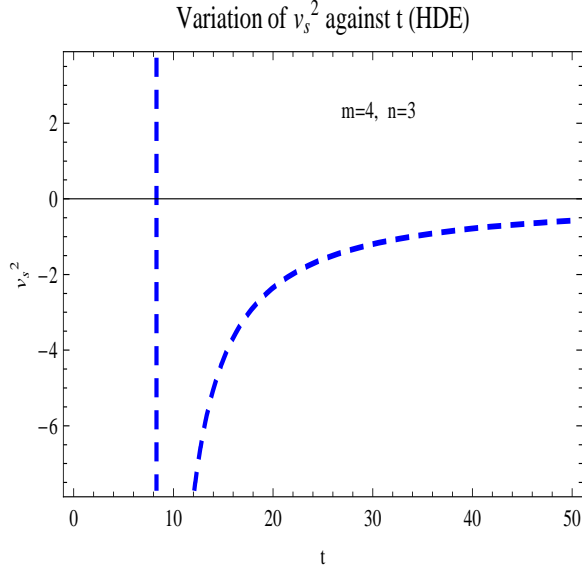


Fig.3

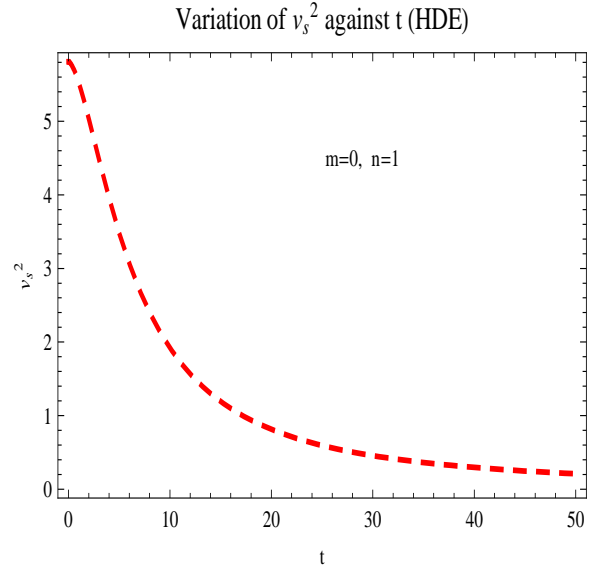


Fig.4

Fig 3, 4 shows the variation of squared speed of sound v_s^2 against time t for HDE dark energy for different values of m and n .

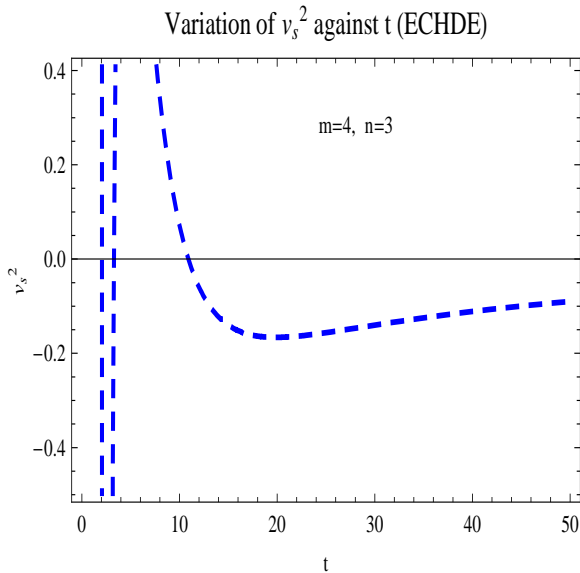


Fig.5

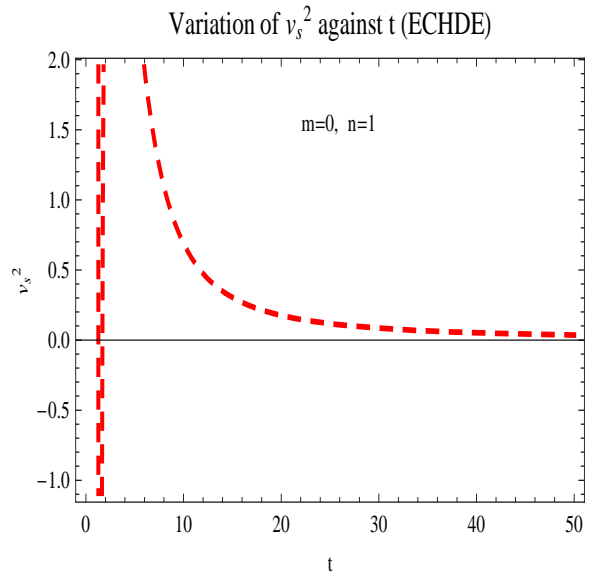


Fig.6

Fig 5, 6 shows the variation of squared speed of sound v_s^2 against time t for ECHDE dark energy for different values of m and n .

- [13] B. Wang et al. :- *Phys. Lett. B* **624** 141 (2005).
- [14] H. Wei et al. :- *Phys. Lett. B* **663** 1 (2008).
- [15] L. N. Granda et al. :- *Phys. Lett. B* **669** 275 (2008).
- [16] M. R. Setare et al. :- *Europhys. Lett.* **92** 49003 (2010).
- [17] H. Wei, R.-G. Cai :- *Phys. Lett. B* **660** 113 (2008).
- [18] C. Gao et al. :- *Phys. Rev. D* **79** 043511 (2009).
- [19] Y. Ling :- *Mod. Phys. Lett. A* **28** 1350128 (2013).
- [20] M. Sharif et. al. :- *Eur. Phys. J. C* **72** 2097 (2012).
- [21] K. Kim et al. :- *Phys. Lett. B* **660** 118 (2008).
- [22] Y. S. Myung :- *Phys. Lett. B* **652** 223 (2007).
- [23] R. Ghosh, U. Debnath :- *Eur. Phys. J. Plus* **129** 81 (2014).
- [24] Z.-P. Huang, Y.-L. Wu :- *JCAP* **07** 035 (2012) *arXiv:1205.0608 [gr-qc]*.
- [25] S. Capozziello, V. F. Cardone, S. Carloni, A. Troisi :- *Int. J. Mod. Phys. D* **12** 1969 (2003).
- [26] S. Nojiri, S. D. Odintsov :- *Gen. Relativ. Gravit.* **36** 1765 (2003).
- [27] A. A. Starobinski :- *Phys. Lett. B* **91** 99 (1980).
- [28] T. P. Sotiriou, V. Faraoni :- *Rev. Mod. Phys.* **82** 451 (2010).
- [29] A. D. Felice, S. Tsujikawa :- *Living Rev. Rel.* **13** 3 (2010).
- [30] G. Cognola, E. Elizalde, S. Nojiri, S. D. Odintsov, L. Sebastiani, S. Zerbini :- *Phys. Rev. D* **77** 046009 (2009)
- [31] E. Elizalde, S. Nojiri, S. Odintsov, L. Sebastiani, S. Zerbini :- *Phys. Rev. D* **83** 086006 (2011).
- [32] S. Nojiri, S. D. Odintsov :- *J. Phys. A* **40** 6725 (2007)